Analysis of α Centauri A&B : The 3D hydrodynamical Approach

L.Bigot[1], F. Thévenin[1], P. Kervella[2]

1-Département Cassiopée, UMR CNRS 6202, Observatoire de la Côte d'Azur, BP 4229, 06304 Nice, CEDEX 4, France
2-LESIA, UMR 8109, Observatoire de Paris-Meudon, 5, place Jules Janssen, F-92195 Meudon Cedex, France

Introduction

The Alpha centauri system is a reference in stellar physics. The two components, Alpha Cen A (G2V) and Alpha Cen B (K1V), have been extensively studied because of their proximity (1.3pc) and similarity to the Sun. The proximity, binarity, presence of solar-like oscillations (Bouchy & Carrier 2002) and since recently possibility to resolve their angular diameters by new generation of interferometers (e.g. VLTI, VINCI+AMBER, Kervella et al. 2003, Bigot et al. 2006) make this system one of the best contrained. It is then particularly interesting for testing both stellar evolution and atmospheric models and study physical processes at work in stars other than the Sun. Its chemical composition has been extensively studied over the past decades. It is known to be a metal-rich system but its overabundance is still debated (from 0.1 dex to 0.25 dex). This amplitude is a serious source of uncertainty in stellar evolution models and therefore in asteroseismic diagnostics. In respect to this problem we decided to improve the determination of its chemical composition by 3D hydrodynamical simulations of their atmospheres. In this poster we present preliminary results for the component A. We found significant smaller overabundances (~0.16 dex). We explore consequences of these new metallicities in terms of splitting of eigenmodes by re-analyzing the work of Thévenin et al. (2002). We also apply our 3D simulation of α Cen B to derive a very accurate radius by fitting new interferometric measurements made at the VLTI.

3D hydrodynamical atmospheric models

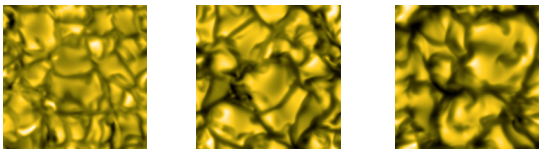

***Fig1**: Disk-center surface intensities of **αCenB(left), Sun (middle) and αCenA (right)** at representative times of their simulations. The dimensions are 6000x6000 kms. The smaller is the the gravity, the larger is the size of granules.*

The numerical code used for this work belongs to a new generation of 3D stellar atmospheric codes originally developed for the study of solar and stellar granulation (e.g. Nordlund 1982, Nordlund & Dravins 1990, Stein & Nordlund 1998) and line formation (e.g. Asplund et al. 2000). The code solves the non-linear, compressible equations of mass, momentum, and energy conservation on a Cartesian mesh. It uses a realistic equation-of-state and opacities (Gustafsson et al. 1975 + updates). The radiative cooling/heating is obtained by solving a pseudo 3D radiative transfer at each time step along several inclined rays (2 in latitude, 4 in longitude, 1 vertical) assuming LTE. The line-blanketing is taken into account through the opacity binning of Nordlund (1982). We use the new ODF from Castelli & Kurucz (2004). Horizontal periodic boundary conditions and transmitting vertical boundaries are used.

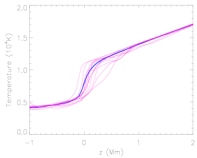

***Fig2**: Spatially resolved temperature profiles in upflows and downflows in αCenA. The thick line represents the horizontal and time averaged temperature.*

We have obtained **time-depent 3D models of the surface layer of Alpha Cen A&B.** The time sequence cover several hours of stellar time enough to cover several convective turn-overs. We used a grid of sufficiently high resolution (x,y,z) = 253x253x163 to get accurate line profiles. The geometrical sizes are 6 x 6 x 5 Mm and are enough to include enough granules. Our models assume: : **Teff (cenA) = 5780 ± 20 K log g (cenA) = 4.32 and Teff (cenB)= 5230 ± 20 K log g (cenB) = 4.50.** We note that Teff is not an input but rather an output slowly varying in time. The input parameter is the entropy of the incoming flow from the bottom of the domain.

We found the same behaviour as in Nordlund & Dravins (1990), i.e. the temperature gradients at the surface are steeper in 3D than in 1D, an effect caused by the strong temperature dependence of H minus and temperature inhomogeneities (granules).

We improve Nordlund & Dravins (1990) simulations of α Cen A&B by using much better grid resolution (32³ in Nordlund & Dravins), *compressible* hydrodynamics (instead of anelastic), newer opacities and ODF's (more than 300 giant lines instead of 42) which are all crucial for accurate abundance determination.

Observations, data reduction and [Fe/H] determination

The observation of α Cen A&B were carried out with the HARPS spectrograph installed on the ESO's 3.6m telescope at La Silla. The data which cover a wavelength region in the visible (380-690nm) were collected during 9 nights (A) and 4 nights (B) of observations in 2003 during the commissioning of the intrument and were kindly provided by F. Bouchy. The large resolution (R = 110000) and high S/N ratio (> 500) are particularly well adapted for abundance determination.

The continuum windows were selected by comparison with the Fourier Solar Telescope (FTS, Brault & Neckel, 1987). The mean level was obtained by a low order spline fit through the selected points. The line list is taken from Asplund et al. (2000). We rejected those which were apparently blended. The oscillator strengths are laboratory measurements provided by the NIST data base and have very good accuracies (<7%). For each line we have calculated several profiles for 4 abundances (7.45 to 8.05) and 5 vsini values (0 to 6 km/s). For each line, [Fe/H] and vsini are found by χ^2 minimization.

Our result show **an abundance of [Fe/H]= 7.61 ± 0.05 dex,** i.e an overabundance with respect to the Sun Δ[Fe/H] = +0.16 dex which is **lower** than the value commonly found in the litterature : Edvardsson et al. (1993) (+ 0.20dex), Neuforge-Verheecke & Magain, 1997 (+0.25dex), Thévenin et al. (2002) (+0.22dex).

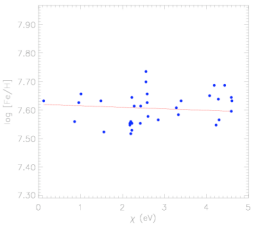

***Fig5**: Individual abundances of FeI lines as a function of the excitation potential for alpha Cen A.*

We note that our value is somewhat larger than Doyle et al. (2005) (+0.11dex) who used 1D models. The projected rotation velocity **vsini is 2.9 ± 0.5 km/s**, in good agreement with the value of 2.7 found by Saar & Osten (1997). Using the radius found by Kervella et al. (2003) and the inclination angle of Pourbaix et al. (1999) we derived a rotation period of 21 ± 4 days.

Application to the interferometry of α CenB

We use new interferometric visibility measurements of αCen B (Bigot et al. 2006) obtained with the VINCI instrument at VLTI in the K band. For the first time, visibility points were obtained in the second lobe which gives a very strong constraint on the limb-darkening.

We compute a series of intensity I(μ) from 3D simulations. Squared visibilities as shown in fig. 7. are obtained after averaging the instrument response in the K band. The fit is obtained by standard χ^2 minimization. We compute limb darkening from 3D hydro, 1D hydrostatic and uniform disk.

The **best agreement is obtained from 3D hydro**.

Assuming a parallaxe π = 747.1 ± 1.2 mas, we have obtained **R = 0.863 ± 0.003 R$_\odot$** whereas 1D (ATLAS) code gives R = 0.865 ± 0.003 R$_\odot$ (0.7σ larger than the 3D prediction).

We note however that for such cool star, the 3D corrections are small in the K band interferometry.

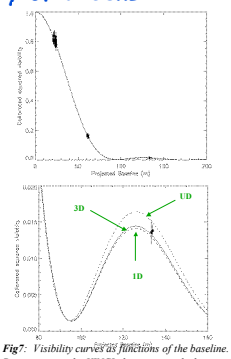

***Fig7**: Visibility curves as functions of the baseline. Dots represent the VINCI observations, the lines correspond to the best theoretical fits.*

Disk integrated synthetic profiles

From the RHD simulation we extract a run of 1 hour of stellar time with snapshots stored every 5min. For each of them, the radiative line transfer equation was solved for several inclined rays assuming LTE. We use the most recent quantum mechanical calculations of hydrogen collisions with neutral species (Anstee & O'Mara 1995, Barklem & O'Mara 1997) which is a great improvement compared with the traditional Unsöld recipe (no need of enhancement factor!).

The flux profiles at different velocities (δv= δλ/λ.xc) were computed as

$$F(v) = \int_{\varphi=0}^{2\pi} \int_{\mu=0}^{1} I(v - v_{rot} \sin i \sin\theta \cos\varphi, \mu, \varphi)\mu \, d\mu \, d\varphi$$

with μ=cos θ. The angular integrals were calculated using a 4 points Gaussian quadrature for μ and 4 equidistant φ angles. The synthetic profiles were convolved with a Gaussian function representing the instrumental profile. The calculated wavelengths are shifted to take into account the gravitational redshift. Finally, the rotationally broadened and convolved profiles for the individual snapshots were added together before normalization to the continuum.

Fig 3. Illustrates the large variety of line profiles formed in a inhomogenous medium. The differences in line strengths and shifts between up- and down-flows are very significant and are responsible for asymmetries.
Fig 4. shows the excellent agreement between the synthetic and observed profiles **without the use of tuned parameters (micro- macro-turbulences),** one of the main advantage of the 3D hydro approach **!**

As noted by Dravins & Nordlund (1990), even if α Cen A is very similar to the Sun in Teff, it is sligthly more evolved and it has therefore a lower surface gravity. This leads to a more vigourous overshoot and sligthly larger velocities in the upper layers which particularly affects the line cores.

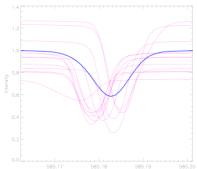

Fig3: *Spatially resolved disk center (μ=0) profiles. The various profile behaviours reflect the variety of temperature profiles in up- and down-flows (cf fig2.). The spatially average is shown as full line.*

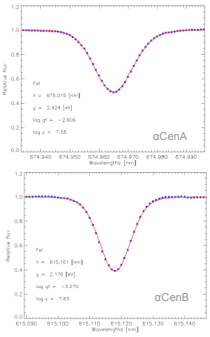

***Fig4**: Comparison between observed (•) and synthetic (—) profiles.*

Application to the asteroseismology of αCenA

The new abundance derived for αCenA is used to re-analyze the paper of Thévenin et al. (2002). For this poster we assume that all changes of abundances scale like [Fe/H]. The new metallicity is Z= 0.0253.
We compute evolutionary models using CESAM code (Morel 1997). The input parameters are : M=1.100M$_\odot$ and R=1.224 ± 0.003 R$_\odot$. Because of its lower metallicity we had to change helium content and the age (6.15 Gy) in order to put the model into the right error bars in the HR diagram.

The oscillation frequencies ν were calculated for various radial and longitudinal nodes (n,l) using a standard pulsation code that solves the problem of linear perturbations of the adiabatic hydrodynamic equations.

We compare predicted large separations $\Delta\nu_{n,l} = \nu_{n+1,l} - \nu_{n,l}$ and small separations $\delta\nu_{n,0,2} = \nu_{n,0} - \nu_{n-1,2}$ with the seimic observations of Bazot et al. (2007). The first scales as $(M/R^3)^{1/2}$ and is a good indicator of the mean density of the star. The small separation is very sensitive to the physical conditions encountered in the stellar core and provide good constrains on the age of the star. As seen in Fig 6., we see that our new model based on new metallicity leads to a good fit of *both* small and large separations.

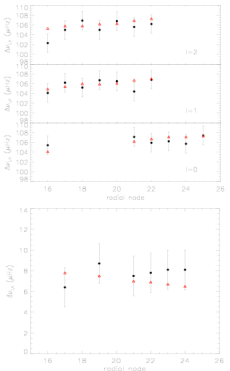

***Fig6**: Large (up) and small (down) separations of α Cen A as function of the radial node. The black points are observed data from Bazot et al. The triangles are theoretical separations.*

Conclusions

The preliminary results based on 3D hydrodynamical simulations presented in this poster show that the overabundance of iron in the solar twin α Cen A is lower than commonly found, only +0.16 dex. This new abundance leads to a very good fit of pulsation data which is very encouraging. In the forthcoming paper (Bigot et al., *in prep*) we will do the same analysis of its companion, α Cen B (preliminary calculations show the same tendency), use more lines and elements (Fe, Si, Ti, Ca, Cr, Ni, O, …) and constrain both evolutions of stars A & B simultaneously. We also used our simulations to fit interferometric data made at VLTI in the case of α Cen B. It led to a very accurate radius.

References

•Anstee S. D., O'Mara B. J., 1995, MNRAS, 276, 859
•Asplund M., Nordlund A., Trampedach R., Allende Prieto C., Stein R. F., 2000, A&A, 359, 729
•Barklem P. S., O'Mara B. J., 1997, MNRAS, 290, 102
•Bazot M., Bouchy F., Kjeldsen H., Charpinet S., Laymand M., Vauclair S., 2007, A&A, 470, 295
•Bigot, L.; Kervella, P.; Thévenin, F.; Ségransan, D., 2006, A&A, 446, 635.
•Bigot, L., Thévenin F., et al., *in prep* for A&A
•Brault J., Neckel, H., 1987, Spectral Atlas of solar disk-averaged and disk-center intensity from 3290 to 12510 (unpublished)
•Castelli F., Kurucz R., astro-ph/0405087
•Doyle, Marianne T., O'Mara, Bernard J., Ross, John E., Bessell, Michael S, 2005, PASA, 22, 6.
•Dravins, D. & Nordlund, A., 1990, 228, 203
•Edvardsson B., Andersen J., Gustafsson B., Lambert D.L., Nissen P.E.,Tomkin J., 1993, A&A 275, 101
•Gustafsson, B.; Bell, R. A.; Eriksson, K.; Nordlund, A., 1975, A&A, 42, 407
•Kervella, P., Thévenin, F., Ségransan, D., et al. 2003, A&A, 404,1087
•Morel, P., 1997, A&AS,124,597
•Neuforge-Verheecke, C. & Magain, P., 1997, A&A, 328, 261
•Nordlund, A. & Dravins, D., 1990, 228, 155
•Nordlund A., A&A, 1982, 107, 1
•Pourbaix, D., Neuforge-Verheecke, C., & Noels, A. 1999,A&A,344, 172
•Saar, S. H. & Osten, R. A. 1997, MNRAS, 284, 803
•Stein R.F. & Nordlund A., 1998, ApJ, 499, 914
•Thévenin, F., Provost, J., Morel, P., Berthomieu, G., Bouchy, F., Carrier, F, 2002, A&A, 392L, 9